electronics

MDPI

Article

Synchronization Mechanism for Controlled Complex Networks under Auxiliary Effect of Dynamic Edges

Lizhi Liu [1,2,*], Zilin Gao [3] and Yi Peng [4]

[1] School of Electric Power Engineering, South China University of Technology, Guangzhou 510641, China
[2] Hunan Institute of Science and Technology, School of Information Science and Engineering, Yueyang 414006, China
[3] School of Computer Science and Engineering, Chongqing Three Gorges University, Wanzhou 404020, China; zilingao@sanxiau.edu.cn
[4] School of Automation, Guangdong University of Technology, Guangzhou 510006, China; pengyi@gdut.edu.cn
* Correspondence: liulizhi94@hnist.edu.cn

Abstract: The scope of complex dynamical networks (CDNs) with dynamic edges is very wide, as it is composed of a class of realistic networks including web-winding systems, communication networks, neural networks, etc. However, a classic research topic in CDNs, the synchronization control problem, has not been effectively solved for CDNs with dynamic edges. This paper will investigate the emergence mechanism of synchronization from the perspective of large-scale systems. Firstly, a CDN with dynamic edges is conceptualized as an interconnected coupled system composed of an edge subsystem (ES) and a node subsystem (NS). Then, based on the proposed improved directed matrix ES model and expanded matrix inequality, this paper overcomes the limitations of coupling term design in node models and the strong correlation of tracking targets between nodes and edges. Due to the effect of the synthesized node controller and the auxiliary effect of the ES, state synchronization can be realized in the CDN. Finally, through simulation examples, the validity and advantages of our work compared to existing methods are demonstrated.

Keywords: state synchronization; complex dynamical networks; edges subsystem; node subsystem

Citation: Liu, L.; Gao, Z.; Peng, Y. Synchronization Mechanism for Controlled Complex Networks under Auxiliary Effect of Dynamic Edges. *Electronics* **2024**, *13*, 1990. https://doi.org/10.3390/electronics13101990

Academic Editor: Martin Reisslein

Received: 16 April 2024
Revised: 10 May 2024
Accepted: 15 May 2024
Published: 20 May 2024

1. Introduction

As a widely observed natural phenomenon, synchronization has attracted a lot of attention in research on complex dynamic networks (CDNs) control. In this field of research, synchronization is regarded as a collective dynamic behavior, and the main concern is identifying a control method that can consistently determine the states between nodes. Previous theoretical results have revealed the existence of laws of the expected dynamic characteristics of complex network systems, and these laws have been applied to social networks, communication networks, multi-intelligent systems, and other fields [1–3].

According to mathematical graph theory, nodes are the carriers of synchronization behavior, while edges (i.e., the topology) play the role of communication bridges between nodes to promote or hinder the emergence of synchronization [1]. In the current research on synchronization in CDNs, exploring the impact of topology (edges) on the node state is the main research direction. Some scholars have explored what conditions of the adjacency matrix (topology) of CDNs are most beneficial for synchronization to occur. For example, the mathematical expressions of the occurrence of synchronization phenomena have been derived under constant topologies [4–7], switching topologies [8–11], and random topologies [12–14]. In Refs. [4–7], the connections between nodes were constant, and the favorable characteristic conditions for synchronous evolution were derived. In Refs. [8–11], the studied CDNs contained multiple topologies, and topology switching was found to follow a certain switching signal. The main purpose of these studies was to identify the topological features and switching frequencies that can assist in the achievement of synchronization. In Refs. [12–14], the

connection or disconnection between nodes followed a given random probability distribution; therefore, exploring the network size and information dissemination patterns can help realize synchronization in such a scenario. Another group of scholars has utilized optimization methods and models of CDNs to seek an optimal topology that can promote synchronization [15–17]. Ref. [15] explored what conditions the spectrum of the topology's Laplacian matrix must satisfy to achieve the optimal synchronizability in high-order complex networks. In Ref. [16], researchers found that a non-trivial and ideal balance between relative connection strengths can lead to network support for optimal collective behavior. In Ref. [17], an optimal power-grid topology with maximum anti-correlation that can drive distributed power grid synchronization was obtained based on the defined frequency correlation function between nodes. Although the diversity of edges and the impact of different topologies on CDNs have been addressed, the dynamic edge group has not been regarded as a dynamic system in the emergence mechanism of synchronization.

In reality, there are many networks where the edges between nodes cannot be described by constant topologies, switching topologies, or random topologies. Edges, like nodes, have rich dynamic characteristics and are generally characterized as dynamic systems. For instance, in industrial web-winding systems, if the motors and the webs between motors are abstracted as nodes and edges, respectively, the motor speed and web tension can be regarded as state variables. A dynamic system of the webs' tension (i.e., the edges' states) can be established based on actual production equipment, and an underactuated control method for motors can be used to make the web tension reach the target value [18,19]. A web-winding system is a typical complex system with dynamic edges, where the coupling relationship between the states of nodes and edges is the source of complex dynamic behavior. It should, thus, be noted that exploring the dynamic characteristics of one aspect of this system depends on the other.

In TCP congestion control, terminal devices such as routers act as nodes for information exchange through transmission links. In order to achieve maximum resource utilization, it is necessary to design reasonable dynamics for the links' prices (i.e., the edges' states) [20,21]. In biological neural networks, the facilitation of synapses can be seen as dynamic behavior of edges, where the adaptability of synaptic dynamics leads to the emergence of chaotic dynamic behaviors [22,23]. In transportation networks, reasonable paths (edges) are crucial for the stable operation of the transportation network [24,25]. In Ref. [24], a Pareto-optimal algorithm was used to solve for the optimal set of each demand node, generating an optimal path that meets the expected travel time and degree of reliability in stochastic transportation networks. Ref. [25] designed an elastic deep learning architecture that solves the problem of sensor placement and traffic flow estimation, then derives a meaningful relationship between traffic flow data and network topology, providing an effective tool for revealing the significance of topology in the stable operation of traffic networks. Ref. [26] emphasized the importance of node dynamics, control protocols, and network topology for the overall behavior of complex networks—in particular, discussing the design method of time-varying coupling protocols in network synchronization. These practical systems indicate that the dynamic changes within edges are sources of dynamic behaviors in networks, especially when designing appropriate edge dynamics that can promote the achievement of desired features in complex networks.

From the above examples of networks, it can be seen that edges can exhibit desired dynamic characteristics, as well as serve a coupling role, so they cannot be simply described using constant, switching, or random modes. Therefore, the dynamic coupling relationship between edges and nodes should be paid more attention to from a holistic perspective. It is necessary to explore the role of edges in the evolution of node states or in effective control methods by establishing an appropriate complex network model. The approach of treating edges as dynamic systems not only expands the existing modeling methods in complex network research but also helps us to understand the essence of dynamic network behavior as a whole. However, research on edge system modeling and corresponding control methods is rare in the existing literature about CDN synchronization control.

From the perspective of large-scale system theory, a complex network can be decomposed into two subsystems composed of nodes and edges, namely the node subsystem (NS) and the edge subsystem (ES). On this basis, an interconnected model of CDNs consisting of NSs and ESs is established [27–32]. The dynamic behaviors of the nodes and edges under the coupling relationship between the two subsystems have been studied. Refs. [27–29] explored the dynamic characteristics of edges, which are rarely addressed, and the edge state tracking control problem was solved using an underactuated node control strategy. Ref. [27] utilized heterogeneous controlled nodes to indirectly drive edge states and derived the correlation between the ES's state and network structure balance. In Ref. [28], controllers of the ES and NS were designed based on the proposed edge-state observer, and the asymptotic tracking of the reference target was achieved under the mutual coupling effect. In Ref. [29], by transferring and expanding the model following a control method based on control theory, model following of the two subsystems was achieved. In order to make nodes exhibit the expected dynamic behavior, a control design method combining edge dynamics was studied in [30–32]. Ref. [28] established a dynamic edges model in discrete-time CDNs and studied design methods of controller and edge dynamics that facilitate synchronization. In Refs. [30,31], a control design method for achieving target tracking of nodes was discussed via the auxiliary role of the ES with and without edge-state observers. Although the modeling problem of dynamic edges and the mutual coupling dynamic behaviors between two subsystems have been investigated, the studies reported in [27–32] have shortcomings in terms of model universality and control design methods that urgently need to be resolved through further studies.

By analyzing the literature, the following two noticeable gaps emerge: (1) In the existing research on CDN synchronization control, the synchronization mechanism of CDNs with dynamic edges is largely ignored [4–17]. This neglect is reflected not only in the dynamic edges' characteristics but also in the impact of edges on node states. (2) There is a lack of universality in the ES models and the design mechanism of synchronization controllers. In Refs. [27–29,31,32], the edge models were in undirected or special vector form, and the controller design method was limited by pre-set coupling structures. In view of these gaps, this paper proposes a more general directed matrix model of dynamic edges based on related works. From the perspective of two subsystems, the synchronization mechanism of controlled CDNs under the auxiliary effect of dynamic edges is investigated.

Compared with most of the existing literature on the synchronization of CDNs, our work provides the following contributions and novelties:

(1) Following the notion of large-scale system control theory, a CDNs is regarded as an interconnected system composed of an NS and an ES. We propose an improved undirected matrix ES model that is more general and realistic than similar models proposed in [27–29,31,32].

(2) Based on the proposed extended matrix inequality lemma, the design mechanism of the synchronization controller and coupled term is simplified, overcoming the limitations of the node model concerning the number of nodes and the tracking-target relationship between the ES and NS in [29,31,32].

The remainder of this paper is organized as follows. Section 2 presents the network model, necessary preliminaries, and proof of the extended matrix inequality lemma. Section 3 discusses the emergence mechanism of synchronization, solves the design problems of the controller and coupling term in this paper, and proves the effectiveness of the design method via the Lyapunov direct method. In Section 4, we provide three examples to compare with existing methods, and the simulation results demonstrate the effectiveness and superiority of our method. Conclusions are drawn in Section 5.

2. Model Description and Preliminaries

Let $x_{ij}(t) \in R$ indicate the time-varying connection weight (edge) from node i pointing to node j at time t. Motivated by the models in [27,28], the dynamics of edges in a CDN with N nodes are proposed as follows:

$$\frac{dx_{ij}(t)}{dt} = \sum_{k=1}^{N} l_{ik}x_{kj}(t) + \sum_{r=1}^{N} l_{jr}x_{ir}(t) + \varphi_{ij}(y(t)), i, j = 1, 2, \cdots, N, \tag{1}$$

where $y(t) = (y_1^T(t), y_2^T(t), \cdots, y_N^T(t))^T \in R^{Nn}$, $y_i(t) \in R^n$ is the state variable of the i-th node, l_{ik} and l_{jr} are real constant coefficients and indicate the strength of the interaction, and $\varphi_{ij}(y(t))$ is the coupling term about nodes' states.

Letting $X(t) = [x_{ij}(t)]_{N\times N}$, $L = [l_{rs}]_{N\times N}$, and $\Phi(y(t)) = [\varphi_{ij}(y(t))]_{N\times N}$, the ES can be described by the following matrix equation:

$$\dot{X}(t) = LX(t) + X(t)L^T + \Phi(y(t)) \tag{2}$$

The state equation of nodes is proposed as follows:

$$\dot{y}_i(t) = f(y_i(t)) + c\sum_{j=1}^{N} x_{ij}(t)h_j(y_j(t)) + u_i(t), i = 1, 2, \cdots, N, \tag{3}$$

where $f(\cdot) : R^n \to R^n$ is a nonlinear function, $c \in R$ is common coupling strength, $h_j(y_j(t)) \in R^n$ is the inner coupled function, and $u_i(t) \in R^n$ is the control input of node i.

Using the Kronecker product, the NS can be described as follows:

$$\dot{y}(t) = F(y(t)) + c(X(t) \otimes I_n)h(y(t)) + u(t), \tag{4}$$

where $F(y(t)) = (f^T(y_1), f^T(y_2), \cdots, f^T(y_N))^T$, $h(y(t)) = (h_1^T(y_1), h_2^T(y_2), \cdots, h_N^T(y_N))^T$, $u(t) = (u_1^T(t), u_2^T(t), \cdots, u_N^T(t))^T$, and $\otimes$ stands for the Kronecker product of the matrices.

Remark 1. *(i) Equation (1) implies that the change in the connection strength (edge state) ($x_{ij}(t)$) is affected by the edges between nodes i and j and the other nodes, as well as the nodes' states. The physical construction of the web-winding system can demonstrate the rationality of Equation (1), in which the change in the tension value of the web (i.e., the edge state) is affected by the adjacent webs and motors (nodes). (ii) The state equation in the form of (2) is employed to govern the dynamics of the ES and investigate the dynamic features of the CDN. However, the models proposed in the the current literature are either of the vector type or are undirected, neither of which can intuitively and realistically represent the variations in dynamic edges. Equation (2) is the improved directed matrix-type edge model proposed in this paper, which is closer to the approach of using adjacency matrices to represent network topology in the existing literature but is not limited by the symmetry of state $X(t)$ (i.e., it is not undirected). (iii) This article aims to reveal the synchronization mechanism of a controlled NS under the auxiliary role of the ES. The achievement of state synchronization relies on an effective controller ($u(t)$) and coupling term ($\Phi(y(t))$). The design method of the coupling term is no longer limited by the node model and the tracking target correlation between the NS and ES. (iv) The asymmetric state matrix ($X(t)$) is not measured accurately by sensors in practical applications, and thus, it is unavailable for the controller ($u(t)$).*

Assumption 1. *The matrix (L) in Equation (2) is Hurwitz stable.*

Assumption 2. *The function $f(\cdot)$ is continuous and satisfies the following condition:*

$$(y_1 - y_2)^T[f(y_1) - f(y_2)] \leq \gamma(y_1 - y_2)^T(y_1 - y_2), \quad for \quad \forall y_1, y_2 \in R^n, \tag{5}$$

where γ is a known positive real number.

Lemma 1 ([33]). *The following properties are true according to the operator $vec(\cdot)$ and the Kronecker product.*

(1) $vec(QWY) = (Q \otimes Y^T)vec(W)$;
(2) $(Q \otimes W)(Y \otimes Z) = (QY) \otimes (WZ)$;
(3) $(Q \otimes W)^T = Q^T \otimes W^T$;
(4) $(Q \otimes W)^{-1} = Q^{-1} \otimes W^{-1}$,

where Q, W, Y, and Z are matrices with appropriate dimensions. The operator $vec(\cdot)$ is defined as $vec(A) = (a_{11}, a_{21}, \cdots, a_{N1}, \cdots, a_{1M}, \cdots, a_{NM})^T$ ($A = [a_{ij}]_{N\times M}$). In property (4) of Lemma 1, matrices Q and W are invertible. A^T and A^{-1} represent the transposition and inverse of matrix A, respectively.

Lemma 2. *If Assumption 1 holds, there is a matrix (Ξ) satisfying the following matrix inequality:*

$$\tilde{L}^T(\Xi \otimes \Xi) + (\Xi \otimes \Xi)\tilde{L} < 0, \tag{6}$$

where $\tilde{L} = L \otimes I_N + I_N \otimes L$.

Proof. If Assumption 1 holds, it follows from matrix theory that there exists a positive definite matrix (Ξ) satisfying the following Lyapunov equation:

$$L^T\Xi + \Xi L < 0. \tag{7}$$

Thus, we can obtain

$$\begin{aligned}(L^T\Xi + \Xi L) \otimes I_N &= L^T\Xi \otimes I_N + \Xi L \otimes I_N \\ &= (L^T \otimes I_N)(\Xi \otimes I_N) + (\Xi \otimes I_N)(L \otimes I_N) < 0,\end{aligned} \tag{8}$$

and

$$\begin{aligned}I_N \otimes (L^T\Xi + \Xi L) &= I_N \otimes L^T\Xi + I_N \otimes \Xi L \\ &= (I_N \otimes L^T)(I_N \otimes \Xi) + (I_N \otimes \Xi)(I_N \otimes L) < 0.\end{aligned} \tag{9}$$

Multiplying $I_N \otimes \Xi$ on the right side of inequality (8), the following can be obtained

$$(L^T \otimes I_N)(\Xi \otimes I_N)(I_N \otimes \Xi) + (\Xi \otimes I_N)(L \otimes I_N)(I_N \otimes \Xi) < 0. \tag{10}$$

It is noticed that $(\Xi \otimes I_N)(L \otimes I_N)(I_N \otimes \Xi) = (\Xi L) \otimes \Xi = (\Xi \otimes \Xi)(L \otimes I_N)$; then, the inequality (10) can be rewritten as follows:

$$(L^T \otimes I_N)(\Xi \otimes \Xi) + (\Xi \otimes \Xi)(L \otimes I_N) < 0. \tag{11}$$

Multiplying $\Xi \otimes I_N$ on the left side of inequality (9), similarly, we can obtain the following inequality:

$$(I_N \otimes L^T)(\Xi \otimes \Xi) + (\Xi \otimes \Xi)(I_N \otimes L) < 0. \tag{12}$$

Obviously, the following inequality can be obtained from (11) and (12):

$$(L^T \otimes I_N + I_N \otimes L^T)(\Xi \otimes \Xi) + (\Xi \otimes \Xi)(L \otimes I_N + I_N \otimes L) < 0. \tag{13}$$

This completes the proof of Lemma 2. □

Remark 2. *(i) There are many systems satisfying Assumption 2, such as Hopfield neural networks, Chua circuits, and so on. (ii) Using Lemma 1, matrix Equation (2) can be transformed into a vector equation to facilitate stability analysis. The proposed extended matrix inequality (6), as evidenced by the theoretical results in Lemma 2, can simplify the design method of coupling term $\Phi(y(t))$,*

overcoming the limitations of the node model and the tracking-target relationship between the NS and ES in [27,29,31,32]. (iii) This paper discusses a synchronous universal control method for CDNs with dynamic edges; the dynamics of the edges and nodes are governed by the proposed models of the ES (2) and NS (4), respectively. The states of edges can indicate whether nodes are connected or not or the strength value of the connection. Thus, the connectivity pattern is actually determined by edges' dynamics, and the number of nodes is not directly related to the proposed methods.

3. Main Results

In this section, we solve the fundamental problem of this paper, namely the design methods of node controllers and coupling terms, to clarify the emergence mechanism of synchronization in CDNs with dynamic edges. In addition, we prove the effectiveness of our proposed design method via the Lyapunov direct method.

Definition 1 ([15]). *A CDN is said to achieve state synchronization if* $\lim_{t\to\infty} y_1(t) = \lim_{t\to\infty} y_2(t) = \cdots = \lim_{t\to\infty} y_N(t) = 0$.

For a CDN consisting of subsystems (2) and (4), we synthesize an effective controller ($u(t)$) and dynamic coupling matrix ($\Phi(y(t))$), making the CDN synchronized. To facilitate an understanding of the synchronization mechanism proposed in this article, we demonstrate the network framework and control diagram in Figures 1 and 2, respectively.

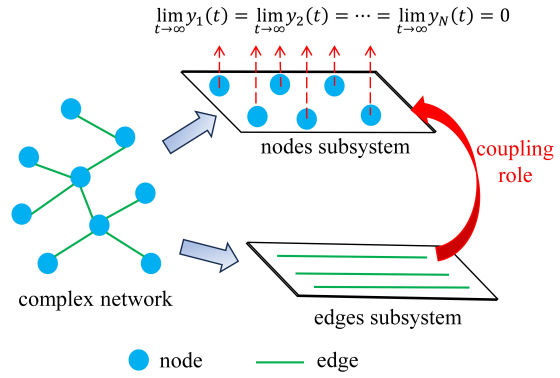

Figure 1. The framework of a CDN composed of an node subsystem (NS) and edge subsystem (ES).

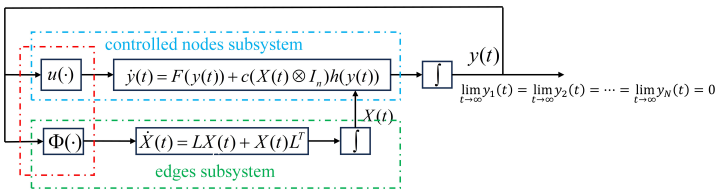

Figure 2. The diagram of a controlled network.

The feedback NS controller is designed as follows:

$$u(t) = (-\alpha - \gamma)(K_\alpha^+ K_\alpha \otimes I_n)y(t), \tag{14}$$

where $K_\alpha = \begin{pmatrix} 1 & -1 & 0 & \cdots & 0 \\ 0 & 1 & -1 & \cdots & 0 \\ \vdots & \vdots & \vdots & \cdots & \vdots \\ 0 & 0 & 0 & \vdots & -1 \\ -1 & 0 & 0 & \cdots & 1 \end{pmatrix} \in R^{N\times N}$, K_α^+ is the Moore–Penrose inverse matrix of K_α, and $\alpha > 0$ is an adjustable scalar and represents the control gain.

The coupling term $\Phi(y(t))$ is constructed as follows:

$$\Phi(y(t)) = -c\Xi^{-1}K_\alpha^T K_\alpha Y(t)\tilde{h}^T(t)\Xi^{-1}, \tag{15}$$

where $\tilde{h}(t) = (h_1(y_1(t)), h_2(y_2(t)), \cdots, h_N(y_N(t)))^T$, Ξ is determined by inequality (7), namely $Y(t) = (y_1(t), y_2(t), \cdots, y_N(t))^T$.

We define the following synchronous errors: $e_i(t) = y_i(t) - y_{i+1}(t)$ $(i = 1, 2, \cdots, N-1)$ and $e_N(t) = y_N(t) - y_1(t)$. Letting vector $e(t) = (e_1^T(t), e_2^T(t), \cdots, e_N^T(t))^T$, according to Lemma 1, the error system reads as follows:

$$\dot{e}(t) = K_\beta \dot{y}(t), \tag{16}$$

where $K_\beta = K_\alpha \otimes I_n$.

In order to carry out stability analysis, the state $(X(t))$ of the ES is vectorized via operator $vec(\cdot)$. Letting $x(t) = vec(X(t)) \in R^{N^2}$, its derivative over time is expressed as follows:

$$\dot{x}(t) = \tilde{L}x(t) - c(\Xi^{-1} \otimes \Xi^{-1})(K_\alpha^T \otimes \tilde{h}(t))K_\beta y(t), \tag{17}$$

Remark 3. *(i) If the error system* (16) *can be asymptotically stable via the node control law* (14) *and coupling term* (15)*, then* $\lim_{t\to\infty}[y_i(t) - y_j(t)] = 0$ *$(i, j = 1, 2, \cdots, N$ and $i \neq j)$ will hold, which is mathematically equivalent to* $\lim_{t\to\infty} y_1(t) = \lim_{t\to\infty} y_2(t) = \cdots = \lim_{t\to\infty} y_N(t) = 0$*. Thus, the synchronization error $(e(t))$ defined in this paper does not contradict the existing literature. (ii) This paper focuses on the synchronization mechanism of a controlled NS under the auxiliary role of the ES. According to the mathematical model of two coupled subsystems, the overall dynamic behavior of the CDN is influenced by the node controller and edge coupling term. Therefore, the fundamental problem that we are aiming to solve is the design of an effective controller $(u(t))$ and coupling term $(\Phi(y(t)))$ that will make the CDN achieve state synchronization.*

Theorem 1. *Consider continuous-time CDNs with mutually coupled subsystems* (2) *and* (4)*. Under Assumptions 1 and 2, synchronization can be realized via the control strategy* (14) *and the coupling term* (15)*; meanwhile, $X(t)$ is bounded.*

Proof. Construct the following positive definite function:

$$V(t) = V_1(t) + V_2(t), \tag{18}$$

where $V_1(t) = e^T(t)e(t)$, $V_2(t) = x^T(t)(\Xi \otimes \Xi)x(t)$, and the positive definite matrix Ξ is solved via inequality (7).

The derivative of $V_1(t)$ can be derived as follows:

$$\begin{aligned}
\dot{V}_1(t) &= 2e^T(t)\dot{e}(t) \\
&= 2e^T(t)K_\beta \dot{y}(t) \\
&= 2e^T(t)K_\beta[F(y(t)) + c(X(t) \otimes I_n)h(y(t)) + u(t)] \\
&= 2e^T(t)K_\beta F(y(t)) + 2ce^T(t)(K_\alpha X(t) \otimes I_n)h(y(t)) + 2e^T(t)K_\beta u(t) \\
&= 2e^T(t)\bar{F}(y(t)) + 2ce^T(t)(K_\alpha X(t) \otimes I_n)h(y(t)) + 2e^T(t)K_\beta u(t),
\end{aligned} \tag{19}$$

where $K_\beta F(y(t)) = \bar{F}(y(t)) = (f^T(y_1) - f^T(y_2), \cdots, f^T(y_{N-1}) - f^T(y_N), f^T(y_N) - f^T(y_1))^T$.

It follows from Assumption 2 that

$$e^T(t)\bar{F}(y(t)) \leq \gamma e^T(t)e(t). \tag{20}$$

From Lemma 1, one has

$$\begin{aligned}(K_\alpha X(t) \otimes I_n)h(y(t)) &= vec(K_\alpha X(t)\tilde{h}(t)) \\ &= (K_\alpha \otimes \tilde{h}^T(t))x(t).\end{aligned} \tag{21}$$

Thus, the following inequality can be obtained via controller (14)

$$\begin{aligned}\dot{V}_1(t) \leq & 2\gamma e^T(t)e(t) + 2ce^T(t)(I_\alpha \otimes \tilde{h}^T(t))x(t) \\ & + 2e^T(t)K_\beta[(-\alpha-\gamma)(K_\alpha^+ K_\alpha \otimes I_n)y(t)] \\ = & -2\alpha e^T(t)e(t) + 2ce^T(t)(K_\alpha \otimes \tilde{h}^T(t))x(t).\end{aligned} \tag{22}$$

The differential coefficient of $V_2(t)$ is derived as follows:

$$\begin{aligned}\dot{V}_2(t) =& \dot{x}^T(t)(\Xi \otimes \Xi)x(t) + x^T(t)(\Xi \otimes \Xi)\dot{x}(t) \\ =& [\tilde{L}x(t) - c(\Xi^{-1} \otimes \Xi^{-1})(K_\alpha^T \otimes \tilde{h}(t))e(k)]^T(\Xi \otimes \Xi)x(t) \\ & + x^T(t)(\Xi \otimes \Xi)[\tilde{L}x(t) - c(\Xi^{-1} \otimes \Xi^{-1})(K_\alpha^T \otimes \tilde{h}(t))e(k)] \\ =& x^T(t)[\tilde{L}^T(\Xi \otimes \Xi)x(t) + (\Xi \otimes \Xi)\tilde{L}]x(t) - 2cx^T(t)(K_\alpha^T \otimes \tilde{h}(t))e(k).\end{aligned} \tag{23}$$

Therefore, we can prove that

$$\dot{V}(t) \leq -2\alpha e^T(t)e(t) + x^T(t)[\tilde{L}^T(\Xi \otimes \Xi) + (\Xi \otimes \Xi)\tilde{L}]x(t). \tag{24}$$

It follows from Lemma 2 that

$$\tilde{L}^T(\Xi \otimes \Xi) + (\Xi \otimes \Xi)\tilde{L} < 0. \tag{25}$$

Therefore, it can be derived that $\dot{V}(t) < 0$ via (24) and (25). Consequently, conclusions about $e(t) \overset{t\to\infty}{\to} 0$ and $X(t) \overset{t\to\infty}{\to} O$ (O denotes the null matrix, and this means that $X(t)$ is stable) can be derived. The proof is accomplished. □

Remark 4. *(i) Matrix K_α is singular, which implies $y(t) \overset{t\to\infty}{\to} 0$ cannot be obtained directly via $e(t) \overset{t\to\infty}{\to} 0$ in Equation (16). Therefore, the synchronization discussed in this article is non-trivial. (ii) The results in Theorem 1 do not indicate that the NS is asymptotically stable. Let $\dot{y}(t) = \Omega y(t) + g(y(t), X(t))$, $\Omega = (-\alpha-\gamma)(K_\alpha^+ K_\alpha \otimes I_n)$, $g(y(t), X(t)) = F(y(t)) + c(X(t) \otimes I_n)h(y(t))$. If matrix Ω is stable and $\|g(y(t), X(t))\| \leq \beta\|y(t)\|$ (where β is an arbitrarily small positive scalar), the stability of the controlled NS can be guaranteed. (iii) The results in Theorem 1 show that the state of the ES (2) is asymptotically stable, which implies the nodes in the network are connected with weak strength when the synchronization of the NS is achieved. The same results are shown in most of the existing literature. In these studies, the structure of the complex network was assumed to satisfy the dissipative condition, in which the interconnected parts in the dynamics of the nodes converge asymptotically to zero in the process of synchronous evolution. Therefore, the results in Theorem 1 are consistent with the existing research. (iv) Based on the form of the node controller in (14) and the coupling term in (15), the design method proposed in this paper can ensure the asymptotic stability of synchronization error ($e(t)$) without being limited by the number of network nodes and is resiliently applicable to CDNs in which the isolated dynamics of nodes are known, are linearizable, or satisfy the Lipschitz condition or the undirected model. (v) The clarity of the synchronization mechanism depends on the effectiveness of the design methods of the node controller and coupling term. The complexity of design methods is related to the degree of difficulty of solving the Moore–Penrose inverse matrix of K_α (K_α^+) and the Lyapunov Equation (7) but is independent of the number of nodes (i.e., network size).*

4. Simulation Examples

4.1. Example 1

Take the following Chua chaotic system [34] as the dynamics of isolated nodes ($N = 30$):

$$\dot{y}_i(t) = Ay_i(t) + g(y_i(t)), i = 1, 2, \cdots, 30, \tag{26}$$

where $y_i(t) = (y_{i1}(t), y_{i2}(t), y_{i3}(t))^T \in R^3$, $g(y_i(t)) = -10(g_1(y_i(t)), 0, 0)^T \in R^3$, matrix $A = \begin{bmatrix} -10 & 10 & 0 \\ 1 & -1 & 1 \\ 0 & -14.87 & 0 \end{bmatrix}$, and $g_1(y_i(t)) = -1.27y_{1i}(t) + 0.295(|y_{1i}(t) + 1| - |y_{1i}(t) - 1|)$.

Let $f(y_i(t)) = Ay_i(t) + g(y_i(t)), \gamma = 9.0620$, the inner coupled functions be $h_i(y_i(t)) = (y_{i1}(t)y_{i2}(t), y_{i2}(t)\ y_{i3}(t), y_{i3}(t)y_{i1}(t))^T$, the control gain be $\alpha = 10$, and the common coupling strength be $c = 0.01$.

Matrices L, Ξ, $y(0)$, and $X(0)$ can be assigned by the following steps:

Step 1. Let $l_i = -m * rand(1), i = 1, 2, \cdots, 30$, where m is an adjustable parameter. We choose $m = 10$, $P \in R^{30\times30}$ as a randomly generated invertible matrix, and $L = Pdiag\{l_1, l_2, \cdots, l_{30}\}P^{-1}$.

Step 2. Let matrix $Q = s * I_N$. The positive matrix (Ξ) can be solved by the equation $L^T\Xi + \Xi L = -Q$, where s is an adjustable parameter and $s = 5$.

Step 3. Set the initial values as $y(0) = randn(90, 1)$ and $X(0) = randn(30)$.

To demonstrate the superiority of the method proposed in our work, the results of a comparison with Ref. [31] are shown in Figures 3–5.

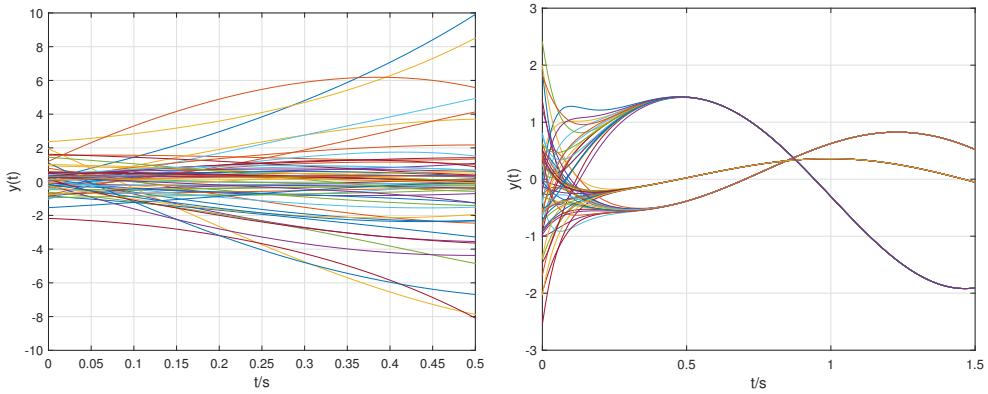

(**a**) (**b**)

Figure 3. The comparison results of NS's state ($y(t)$) response curves in Example 1: (**a**) under the control method proposed in Ref. [31]; (**b**) under the proposed control method.

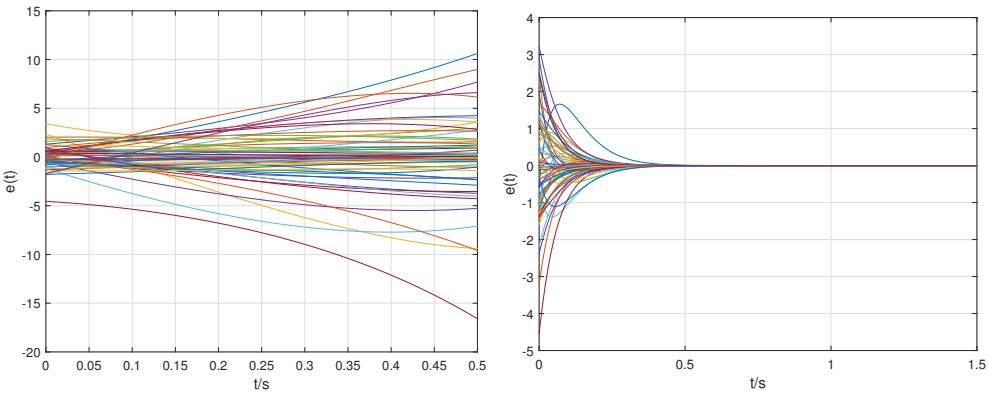

(**a**) (**b**)

Figure 4. The comparison results of synchronization error ($e(t)$) response curves in Example 1: (**a**) under the control method proposed in Ref. [31]; (**b**) under the proposed control method.

4.2. Example 2

Consider a continuous analog Hopfieldneural network [35] consisting of 50 nodes; the dynamic equation of the neuron reads as follows:

$$\dot{y}_i(t) = -\frac{1}{\tau_i}y_i(t) + \frac{1}{C_i}D_i(t) + \frac{1}{C_i}\sum_{j=1}^{N} x_{ij}(t)h_j(y_j(t)), i = 1, 2, \cdots, 50. \quad (27)$$

where the i-th neuron's state is $y_i(t) \in R$, C_i is the input capacitance, $\tau_i = R_iC_i$, R_i is the effective resistance, $D_i(t)$ is the input current, and the activation function is $h_j(y_j(t)) = \frac{1-e^{-y_j(t)}}{1+e^{-y_j(t)}}$.

Let $C_i = C = 1$, $R_i = R = 1$, $c = \frac{1}{C}$, $\tau_i = \tau = \frac{1}{RC}$, $D_i(t) = D(t) = cos(t)$, $f(y_i(t)) = -\frac{1}{\tau}y_i(t) + \frac{1}{C}D(t)$, $(1 \le i \le 50)$, $\gamma = 1$, and $\alpha = 5$. The initial values of $y(0)$ and $X(0)$ and matrices L and Ξ are obtained following Steps 1–3 in Example 1.

The results of the comparison with Ref. [32] are shown in Figures 6–8.

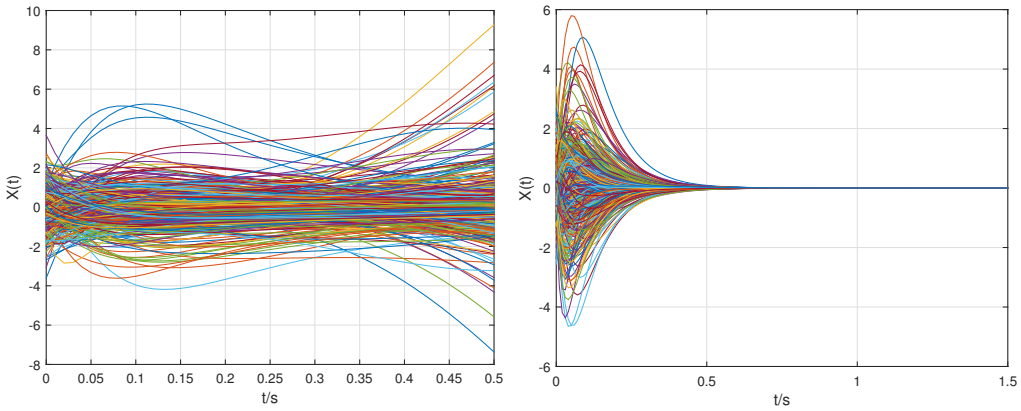

(**a**) (**b**)

Figure 5. The comparison results of ES's state ($X(t)$) response curves in Example 1: (**a**) under the control method proposed in Ref. [31]; (**b**) under the proposed control method.

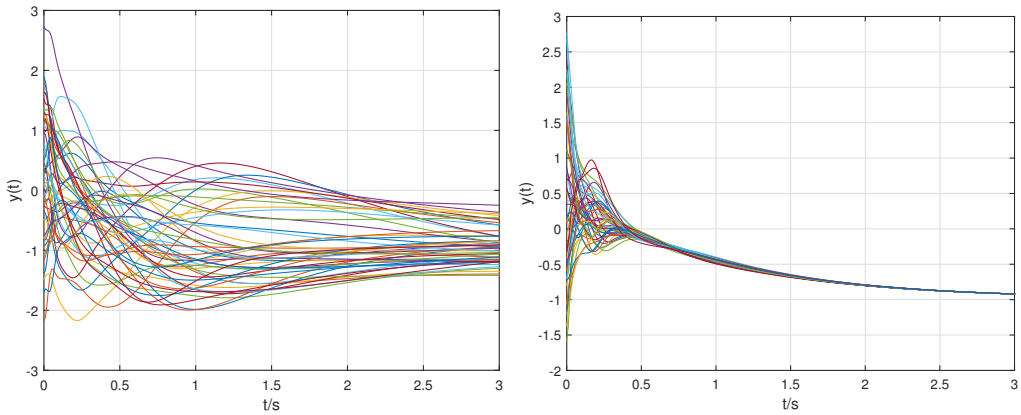

(**a**) (**b**)

Figure 6. The comparison results of NS's state ($y(t)$) response curves in Example 2: (**a**) under the control method proposed in Ref. [32]; (**b**) under the proposed control method.

4.3. Example 3

To further demonstrate the effectiveness of the method proposed in this work in a practical application, we take fixed-wing unmanned aerial vehicles (FWUAVs) as the nodes. As shown in [36,37], the attitude dynamics of the FWUAVs are described as follows:

$$\begin{bmatrix} \dot{y}_{i1}(t) \\ \dot{y}_{i2}(t) \\ \dot{y}_{i3}(t) \end{bmatrix} = \begin{bmatrix} \delta_1 y_{i1}(t) y_{i2}(t) - \delta_2 y_{i2}(t) y_{i3}(t) \\ \delta_3 y_{i1}(t) y_{i3}(t) - \delta_4 (y_{i1}{}^2(t) - y_{i3}{}^2(t)) \\ \delta_5 y_{i1}(t) y_{i2}(t) - \delta_1 y_{i2}(t) y_{i3}(t) \end{bmatrix} + B u_i(t), i = 1, 2, \cdots, 100. \quad (28)$$

where y_{i1}, y_{i2}, and y_{i3} are the roll, pitch, and yaw angular rates of the i-th FWUAV, respectively; $u_i(t)$ is the control input; $B = \begin{bmatrix} \delta_6 & \delta_7 & 0 \\ 0 & 0 & \delta_8 \\ \delta_7 & \delta_9 & 0 \end{bmatrix}$; and $y_i(t) = [y_{i1}, y_{i2}, y_{i3}]^T$ is the state variable.

During the flight of FWUAVs, the states of edges (distance, communication speed, etc.) are constantly changing. We assume that the states of edges between FWUAVs are governed by (2), then verify the effectiveness of the design method.

We set the following parameters: $\delta_1 = 0.001$, $\delta_2 = -0.0107$, $\delta_3 = 0.0107$, $\delta_4 = 0.0103$, $\delta_5 = 0.0102$, $\delta_6 = 0.0181$, $\delta_7 = 0.0030$, $\delta_8 = 0.0004$, and $\delta_9 = -0.0011$. The control input is $u(\tilde{t}) = B^{-1}u(t)$, the inner coupled function is $h_i(y_i(t)) = y_i(t)$, the common connection strength is $c = 0.01$, control gain is $\alpha = 0.5$, and $\gamma = 0.5$. The initial values of $y(0)$ of $X(0)$ and matrices L a d Ξ are obtained via Steps 1–3 in Example 1.

The results of the comparison with Ref. [32] are shown in Figures 9–11.

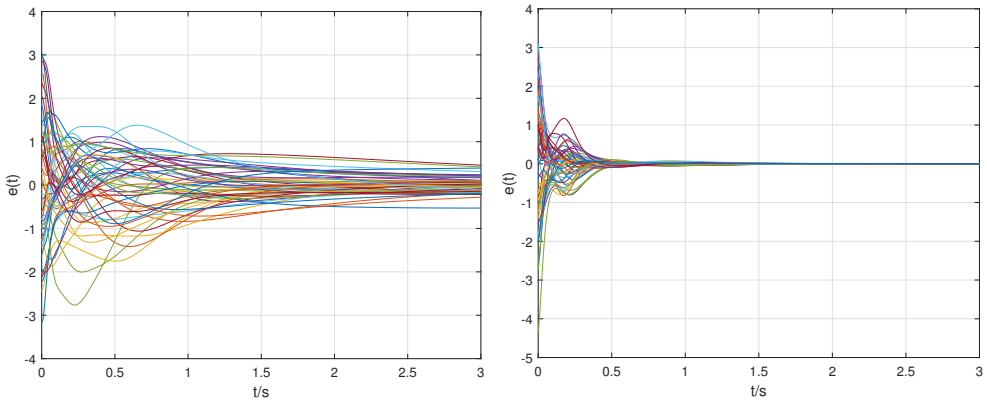

(**a**) (**b**)

Figure 7. The comparison results of synchronization error ($e(t)$) response curves in Example 2: (**a**) under the control method proposed in Ref. [32]; (**b**) under the proposed control method.

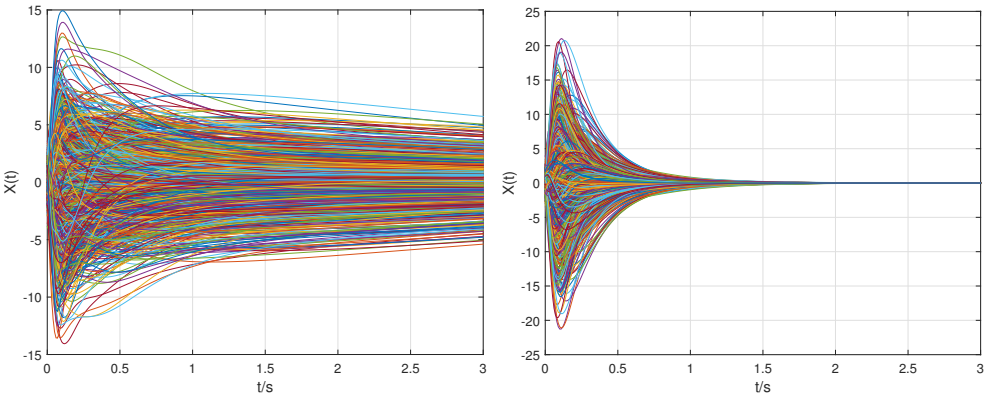

(**a**) (**b**)

Figure 8. The comparison results of ES's state ($X(t)$) response curves in Example 2: (**a**) under the control method proposed in Ref. [32]; (**b**) under the proposed control method.

4.4. Comparative Analysis of Simulation Results

By observing Figures 3–11, the following conclusions can be drawn:

(1) Using the control method proposed in [31,32], the simulation results for the three examples are shown in Figures 3a, 4a, 5a, 6a, 7a, 8a, 9a, 10a and 11a. It can be seen that it is neither possible to drive the NS to achieve asymptotic state synchronization nor to ensure the stability of the states of the ES. However, under the controller and coupling term designed in this article, we can see from Figures 3b, 4b, 6b, 7b, 9a, and 10a that the synchronization error and node state are stable. Compared with [31,32], the results demonstrate the effectiveness and advantages of the method proposed in this paper.

(2) The state of the ES is bounded in Figures 5b, 8b, and 11b, which implies that the interconnected parts of nodes will converge asymptotically to zero. The results are consistent with Theorem 1 and most existing research.

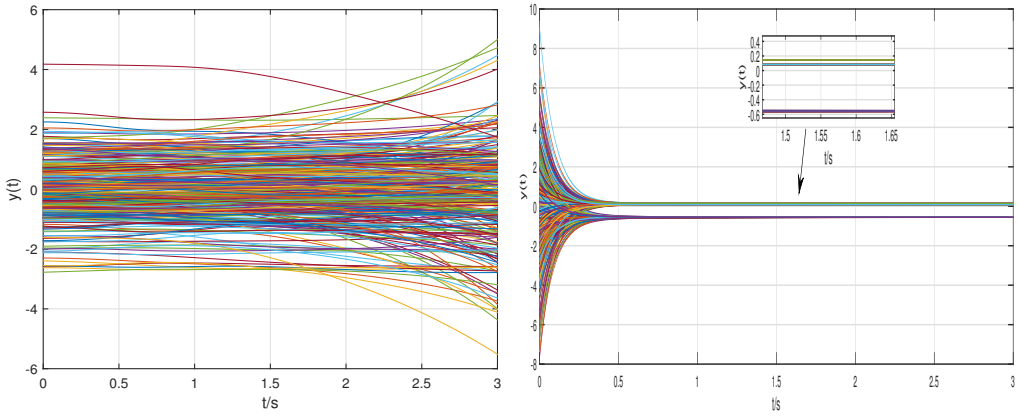

(**a**) (**b**)

Figure 9. The comparison results of NS's state ($y(t)$) response curves in Example 3: (**a**) under the control method proposed in Ref. [32]; (**b**) under the proposed control method.

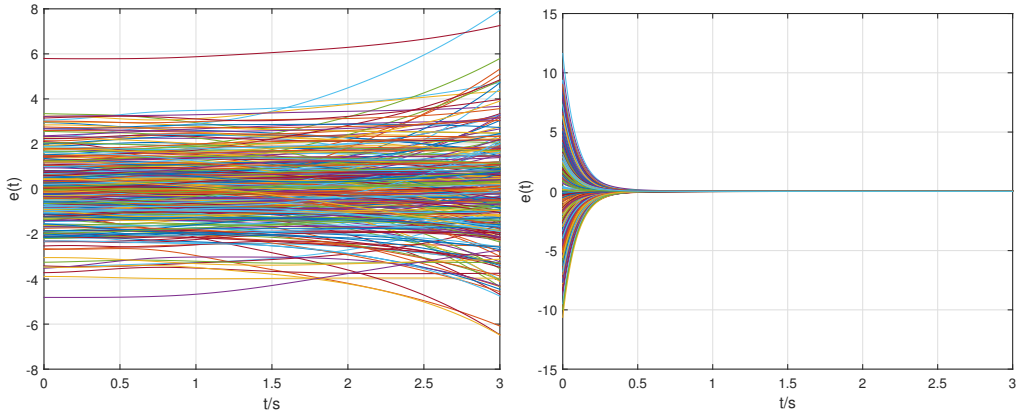

(**a**) (**b**)

Figure 10. The comparison results of synchronization error ($e(t)$) response curves in Example 3: (**a**) under the control method proposed in Ref. [32]; (**b**) under the proposed control method.

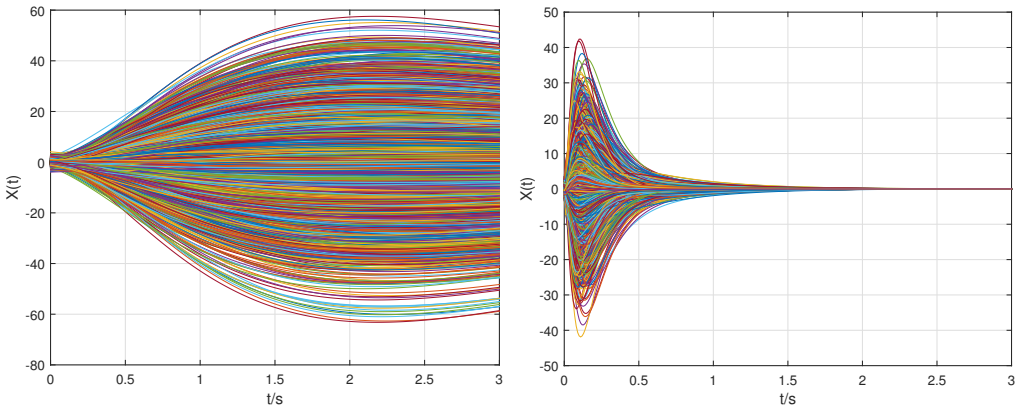

(**a**) (**b**)

Figure 11. The comparison results of ES's state ($X(t)$) response curves in Example 3: (**a**) under the control method proposed in Ref. [32]; (**b**) under the proposed control method.

(3) In this section, we set the number of nodes (N) to 30, 50, and 100 in examples 1, 2, and 3, respectively, and all simulation results indicate that the control objectives can be achieved. Therefore, in both theory and simulation, it has been demonstrated that the method proposed in this paper is not limited by the number of nodes.

5. Conclusions

This paper discusses a synchronization control mechanism for CDNs with dynamic edges. The proposed interconnected coupled model, composed of an ES and an NS, can reveal the auxiliary effect of the ES on the controlled NS and provides a new approach to studying synchronous evolution. Due to the improved matrix ES model and the expanded matrix inequality lemma, the design method of the coupling term is no longer limited by the node model and the associated relationship of the tracking targets between the ES and NS. Moreover, both the theoretical analysis and simulation results of this article prove the effectiveness of the proposed method and its superiority to existing methods. The research findings of this article will contribute to the development of research on the dynamic behavior of CDNs.

In the future, we will expand our research work in the following two areas: (i) Nonlinear ES models and pinning control methods will be developed. This paper mainly discusses the auxiliary mechanism of a linear ES model, assisting in the emergence of synchronization of controlled nodes, without considering nonlinear models of the ES. We will establish a more general nonlinear edge model and use the pinning control method to study the emergence mechanism of synchronization. (ii) A model-free, data-driven method will be developed. Under the unknown models of the ES and NS, the collected complex state information of the CDN and data-driven methods will be used to design control laws and achieve state synchronization.

Author Contributions: Methodology, L.L.; software, Z.G.; validation, Z.G. and Y.P.; writing—original draft preparation, L.L.; writing—review and editing, Z.G. and Y.P. All authors have read and agreed to the published version of the manuscript.

Funding: This work was supported by Scientific Research Fund of Hunan Province Education Department (23B0646), Scientific and Technological Research Program of Wanzhou District (wzstc-20230309), Basic and Applied Basic Research Foundation of Guangdong Province (2024A1515011652).

Data Availability Statement: Data are contained within the article.

Conflicts of Interest: The authors declare no conflicts of interest.

References

1. Boccaletti, S.; Latora, V.; Moreno, Y.; Chavez, M.; Hwang, D.U. Complex networks: Structure and dynamics. *Phys. Rep.* **2006**, *424*, 175–308. [CrossRef]
2. Cao, Y.W.; Maghsudi, S.; Ohtsuki, T.; Quek, T. Mobility-Aware Routing and Caching in Small Cell Networks Using Federated Learning. *IEEE Trans. Commun.* **2024**, *7*, 815–829. [CrossRef]
3. Olfati-Saber, R.; Fax, J.A.; Murray, R.M. Consensus and Cooperation in Networked Multi-Agent Systems. *Proc. IEEE* **2007**, *95*, 215–233. [CrossRef]
4. Xia, Y.; Liu, X. Successive Lag Synchronization for Multilayer Complex Networks with Multiple Weights. *IEEE Trans. Circuits Syst. II Express Briefs* **2023**, *70*, 3514–3518. [CrossRef]
5. Wu, Y.; Guo, H.; Xue, L.; Gunasekaran, N.; Liu, J. Prescribed-Time Synchronization of Stochastic Complex Networks with High-Gain Coupling. *IEEE Trans. Circuits Syst. II Express Briefs* **2023**, *70*, 4133–4137. [CrossRef]
6. Wu, Y.; Sun, J.; Gunasekaran, N.; Kurths, J.; Liu, J. Exponential Output Synchronization of Complex Networks with Output Coupling via Intermittent Event-Triggered Control. *IEEE Trans. Control Netw. Syst.* **2024**, *11*, 284–294. [CrossRef]
7. Xu, Y.; Gao, Q.; Xie, C.; Zhang, X.; Wu, X. Finite-Time Synchronization of Complex Networks with Privacy-Preserving. *IEEE Trans. Circuits Syst. II Express Briefs* **2023**, *70*, 4103–4107. [CrossRef]
8. Du, K.; Ma, Q.; Kang, Y.; Fu, W. Robust Cluster Synchronization in Dynamical Networks with Directed Switching Topology via Averaging Method. *IEEE Trans. Syst. Man Cybern. Syst.* **2022**, *52*, 1694–1704. [CrossRef]
9. Guo, Z.; Xie, H.; Wang, J. Finite-Time and Fixed-Time Synchronization of Coupled Switched Neural Networks Subject to Stochastic Disturbances. *IEEE Trans. Syst. Man Cybern. Syst.* **2022**, *52*, 6511–6523. [CrossRef]
10. Zhai, S.; Wang, X.; Zheng, Y. Cluster Synchronization of a Nonlinear Network with Fixed and Switching Topologies. *IEEE Syst. J.* **2023**, *17*, 6511–6523. [CrossRef]
11. Fu, J.; Li, C.; Huang, Y.; Li, Y.; Chai, T. Invariance Principles for Nonlinear Discrete-Time Switched Systems and Its Application to Output Synchronization of Dynamical Networks. *IEEE Trans. Cybern.* **2024**, *54*, 1261–1271. [CrossRef]
12. Yin, X.; Xiao, R.; Dai, H.; Zhu, Q.; Sun, Y. Influence of Layer Similarity on the Synchronization of Multiplex Networks with Random Topologies. *IEEE Trans. Syst. Man Cybern. Syst.* **2023**, *53*, 7089–7098. [CrossRef]
13. Uwate, Y.; Nishio, Y.; Ott, T. Synchronization of Chaotic Circuits with Stochastically-Coupled Network Topology. *Int. J. Bifurc. Chaos* **2021**, *31*, 2150015. [CrossRef]
14. Zhou, S.; Guo, Y.; Liu, M.; Lai, Y.C.; Lin, W. Random temporal connections promote network synchronization. *Phys. Rev.* **2019**, *100*, 032302. [CrossRef]
15. Chen, G. Searching for Best Network Topologies with Optimal Synchronizability: A Brief Review. *IEEE/CAA J. Autom. Sin.* **2022**, *9*, 573–577. [CrossRef]
16. Tang, Y.; Shi, D.; Lü, L. Optimizing higher-order network topology for synchronization of coupled phase oscillators. *Commun. Phys.* **2022**, *5*, 96. [CrossRef]
17. Li, X.; Wei, W.; Zheng, Z. Promoting synchrony of power grids by restructuring network topologies. *Chaos* **2023**, *533*, 063149. [CrossRef]
18. Dang, V.T.; Nguyen, D.B.H.; Tran, T.D.T.; Le, D.T.; Nguyen, T.L. Model-free hierarchical control with fractional-order sliding surface for multisection web machines. *Int. J. Adapt. Control Signal Process.* **2023**, *37*, 497–518. [CrossRef]
19. Nian, X.; Fu, X.; Chu, X.; Xiong, H.; Wang, H. Disturbance observer-based distributed sliding mode control of multimotor web-winding systems. *IET Control Theory Appl.* **2020**, *14*, 614–625. [CrossRef]
20. Wang, H.; Tang, J.; Hong, B. Research of Wireless Congestion Control Algorithm Based on EKF. *Symmetry* **2020**, *12*, 646. [CrossRef]
21. Zhang, T.; Mao, S. Machine Learning for End-to-End Congestion Control. *IEEE Commun. Mag.* **2020**, *58*, 52–57. [CrossRef]
22. Barrio, R.; Jover-Galtier, J.A.; Mayora-Cebollero, A.; Mayora-Cebollero, C.; Serrano, S. Synaptic dependence of dynamic regimes when coupling neural populations. *Phys. Rev. E* **2024**, *109*, 014301. [CrossRef]
23. Sawicki, J.; Berner, R.; Loos, S.A.; Anvari, M.; Bader, R.; Barfuss, W.; Botta, N.; Brede, N.; Franović, I.; Gauthier, D.J.; et al. Perspectives on adaptive dynamical systems. *Chaos* **2023**, *33*, 071501. [CrossRef] [PubMed]
24. Owais, M.; Alshehri, A. Pareto Optimal Path Generation Algorithm in Stochastic Transportation Networks. *IEEE Access* **2020**, *8*, 58970–58981. [CrossRef]
25. Owais, M. Deep Learning for Integrated Origin–Destination Estimation and Traffic Sensor Location Problems. *IEEE Trans. Intell. Transp. Syst.* **2024**, *early access*, 1–13. [CrossRef]
26. DeLellos, P.; Bernardo, M.; Gorochowski, E.T.; Russo, G. Synchronization and control of complex networks via contraction, adaptation and evolution. *IEEE Circuits Syst. Mag.* **2010**, *10*, 64–82. [CrossRef]
27. Gao, Z.; Guo, C.; Li, Y.; Liu, L.; Luo, W. Stabilization of a structurally balanced complex network with similar nodes of different dimensions. *Appl. Math. Comput.* **2023**, *458*, 128238. [CrossRef]
28. Liu, L.; Wang, Y.; Gao, Z. Tracking control for the dynamic links of discrete-time complex dynamical network via state observer. *Appl. Math. Comput.* **2020**, *369*, 124857. [CrossRef]
29. Li, X.X.; Wang, Y.H.; Li, S.P. Double Model Following Adaptive Control for a Complex Dynamical Network. *Entropy* **2023**, *25*, 115. [CrossRef]
30. Liu, L.; Gao, Z.; Wang, Y.; Li, Y. Stabilization and synchronization control for discrete-time complex networks via the auxiliary role of edges subsystem. *Neurocomputing* **2024**, *568*, 127029. [CrossRef]

31. Gao, P.; Wang, Y.; Liu, L.; Zhang, L.; Li, S. Double tracking control for the directed complex dynamic network via the state observer of outgoing links. *Int. J. Syst. Sci.* **2023**, *54*, 895–906. [CrossRef]
32. Gao, P.; Wang, Y.; Peng, Y.; Zhang, L.L.; Li, S. Tracking control of the nodes for the complex dynamical network with the auxiliary links dynamics. *Inf. Sci.* **2023**, *628*, 350–359. [CrossRef]
33. Barnett, S. Matrix differential equations and kronecker products. *SIAM J. Appl. Math.* **1973**, *24*, 1–5. [CrossRef]
34. Lu, J.; Chen, G. Generating multiscroll chaotic attractors: Theories, methods and applications. *Int. J. Bifurc. Chaos* **2006**, *16*, 775–858. [CrossRef]
35. Hopfiled, J.J.; Tank, D.W. Computing with neural circuits: A model. *Science* **1986**, *233*, 625–633. [CrossRef] [PubMed]
36. Poksawat, P.; Wang, L.P.; Mohamed, A. Gain Scheduled Attitude Control of Fixed-Wing UAV with Automatic Controller Tuning. *IEEE Trans. Control Syst. Technol.* **2018**, *26*, 1192–1203. [CrossRef]
37. Salman, S.A.; Sreenatha, A.G.; Choi, J.Y. Attitude Dynamics Identification of Unmanned Aircraft Vehicle. *Int. J. Control Autom. Syst.* **2006**, *4*, 782–787. [CrossRef]